molbank

MDPI

Communication

A New Synthetic Route for Preparation of 5-Methyl-5-Benzylhydantoin: X-Ray Analysis and Theoretical Calculations

Emiliya Cherneva [1,2], Rossen Buyukliev [1], Boris Shivachev [3], Rusi Rusew [3] and Adriana Bakalova [1,*]

[1] Department of Chemistry, Faculty of Pharmacy, Medical University—Sofia, 2 Dunav Str., 1000 Sofia, Bulgaria; cherneva@pharmfac.mu-sofia.bg (E.C.); buyukliev@pharmfac.mu-sofia.bg (R.B.)
[2] Institute of Organic Chemistry with Centre of Phytochemistry, Bulgarian Academy of Sciences, Acad. G. Bonchev Str., Build. 9, 1113 Sofia, Bulgaria
[3] Institute of Mineralogy and Crystallography, Bulgarian Academy of Science, Acad. G. Bonchev Street, 107 bl, 1113 Sofia, Bulgaria; blshivachev@gmail.com (B.S.); r.rusev93@gmail.com (R.R.)
* Correspondence: a_bakalova@pharmfac.mu-sofia.bg; Tel.: +359-897086067

Abstract: The aim of this study was to use a different synthetic route for the preparation of 5-methyl-5-benzyl hydantoin by modifying the Bucherer–Berg reaction. This different route for the synthesis led to improvement in reaction time, purity of the compound, and practical yield. The synthesized compound was characterized spectroscopically by IR, ^{1}H, ^{13}C NMR, and mass spectrometry. The X-ray diffraction method was used to determine the chemical structure. The experimental data from X-ray analysis were compared with theoretically calculated data by DFT analysis.

Keywords: benzylhydantoin; XRD

check for updates

Academic Editor: Kristof Van Hecke

Received: 11 December 2024
Revised: 15 January 2025
Accepted: 20 January 2025
Published: 22 January 2025

Citation: Cherneva, E.; Buyukliev, R.; Shivachev, B.; Rusew, R.; Bakalova, A. A New Synthetic Route for Preparation of 5-Methyl-5-Benzylhydantoin: X-Ray Analysis and Theoretical Calculations. *Molbank* **2025**, *2025*, M1956. https://doi.org/10.3390/M1956

1. Introduction

Hydantoins are a class of compounds containing a hydantoin substructure as a scaffold. Hydantoins or imidazolidine-2,4-diones are a five-membered heterocycles. Recently, too many reviews have been devoted to the synthesis and pharmacological and biological application of hydantoin derivatives [1–4]. Interest in synthetic methods for the preparation of hydantoins is increasing worldwide due to their widespread use in medicine [5–17]. They have focused on all the methods existing in chemistry, ranging from the first historical reactions of Bilz, Ried, or Bucherer–Berg to the more modern multicomponent reactions (MCR) that have been used to create thousands of hydantoin compounds [18–24]. In 1932, Herbst [25] synthesized 5-methyl-5-benzyl hydantoin and studied it by elemental analyses and melting point. So far, a detailed description of the compound, such as crystal structure, IR, and NMR spectra, has not been published.

In the present study, a new synthetic route for the synthesis of 5-methyl-5-benzyl hydantoin, as well as its spectral investigation and crystal structure, is presented.

2. Results and Discussion

The Herbst method includes the reaction of phenylacetone with ammonium cyanide to 1-amino-1-methyl-2-phenylethanonitril, followed by interaction with potassium cyanate [25]. The obtained urea derivative is acidifying to 5-methyl-5-benzyl hydantoin.

We synthesized 5-methyl-5-benzyl hydantoin by using the Bucherer–Berg reaction, which belongs to the multiple-component reaction. The preparation of the compound was performed by heating an aqueous ethanol solution (1:1) of phenylacetone with sodium cyanide and ammonium carbonate (Scheme 1) at 60 °C. The title compound obtained by the Bucherer–Berg reaction enhanced the reaction time to 24 h as well as the purity and yield until comparable with the Herbst method.

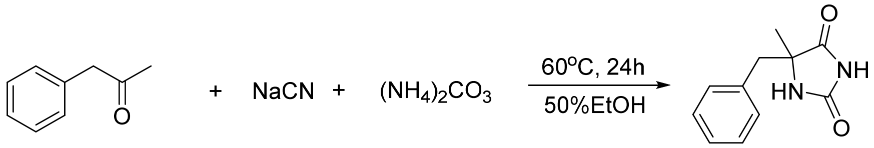

Scheme 1. Synthetic route for preparation of 5-methyl-5-benzyl hydantoin.

In the IR spectrum of the compound, an NH stretching vibration is observed at 3109 cm^{-1}, which corresponds to hydrogen-bonded NH groups. Its calculated frequency (by the DFT method) is in the range of 3535–3520 cm^{-1}. The experimental frequency for the C=O stretcher appears as a strong band at 1748 cm^{-1} and as a shoulder at 1732 cm^{-1}, which is in good agreement with the literature data [26]. The theoretical values for the stretched modes of the C=O groups are at 1791 cm^{-1} and 1755 cm^{-1}. Aromatic C=C and C-H stretching frequencies are observed in the typical aromatic vibrational range (Figure S1).

Two doublets (AB quartet, J = 15.5 Hz) are observed in the ^1H NMR spectra at 3.16 and 2.94 ppm for the diastereotopic CH_2 group protons. The chemical shifts of the aromatic protons are at 7.34, 6.91, and 6.81 ppm. The signals at 7.94 and 10.36 ppm are due to the N-H hydantoin protons (NH-1) and (NH-3). In the ^{13}C spectrum, the signals for the carbonyl groups—C=O-2 and C=O-4 are at 178.0 and 156.6 ppm, respectively. The carbon C-5 of the hydantoin ring is at 63.3 ppm (Figures S2 and S3).

Compound 5-methyl-5-benzyl hydantoin crystallized from 50% ethanol solution in the monoclinic space group *Pn* with two molecules per asymmetric unit (ASU) and a total of four molecules in the unit cell ($Z = 4$, $Z' = 2$, Table S1). ORTEP view [27] of the molecules in the ASU are given in Figure 1a. Values for bond lengths, angles, and torsion angles derived from the structural analysis are given in Tables S2–S4 and are comparable to those of other similar compounds [28–30]. The principal features of the molecular structure of compound 5-methyl-5-benzyl hydantoin include hydantoin, toluyl moieties, and asymmetric (inversion) center at atoms C51 and C52. The difference between the two molecules present in the asymmetric unit is in the rotation of the hydantoin ring around (C7-C5). This is clearly seen from the overlay of the two independent molecules present in the ASU (Figure 1b). The direct overlay of the hydantoin moieties produces an alignment root-mean-square deviation (RMSD) value of 1.632 Å. When inversion is applied, the alignment RMSD value between the moieties is 0.088 Å. The hydantoin moiety is rich in hydrogen bond donors (2 × N-H) and hydrogen bond acceptors (2 × C=O); therefore, the presence of hydrogen bond interactions is anticipated. The strength of the hydrogen bonding interactions depends not only on the specific donor–acceptor combination but also on the hydrogen bond length and bond angles. Therefore, strong hydrogen bonding interactions are considered those with $H \cdots A$ distances less than 2 Å ($D \cdots A$ distances less than 2.8 Å) and D—H···A angles between 170° and 180° [31,32]. Indeed, the crystal structure of 5-methyl-5-benzyl hydantoin is stabilized by four strong intermolecular hydrogen bonding interactions of N-H···O=C type with $H \cdots A$ distances between 1.81 and 1.93 Å and D—H···A angles between 159° and 176° (Figure 2a and Table 1). Moreover, two additional weak hydrogen bonding interactions of C-H···O=C type are detected (C61—H61A···O42 and C61—H61B···O41) with $H \cdots A$ distances between 2.53 and 2.67 Å and D—H···A angles between 137° and 153° (Figure 2a and Table 1). Short intermolecular contacts of C-H. . .C and C-H. . .O type with distances shorter than the *vdW* radii of the involved atoms are also present. Other non-covalent interactions, such as π-π interactions between conjugated systems, are not detected. The combination of hydrogen bond interactions and short contacts defines the specific three-dimensional arrangement of the molecules in the crystal structures. As seen from the projections perpendicular to the *c*-axis and *b*-axis, the molecules of 5-methyl-5-benzyl hydantoin are joined into pseudo layers (Figure 2b,c).

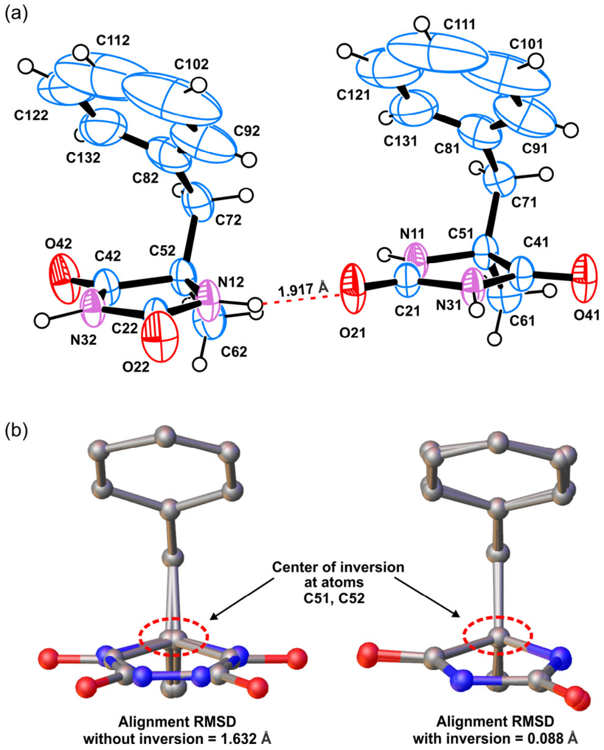

Figure 1. ORTEP view [27] of the molecules in the asymmetric unit (ASU) in the crystal structure of compound X at 50% probability level—(**a**,**b**) overlay of the two independent molecules in the ASU, emphasizing the chirality at atoms C51 and C52.

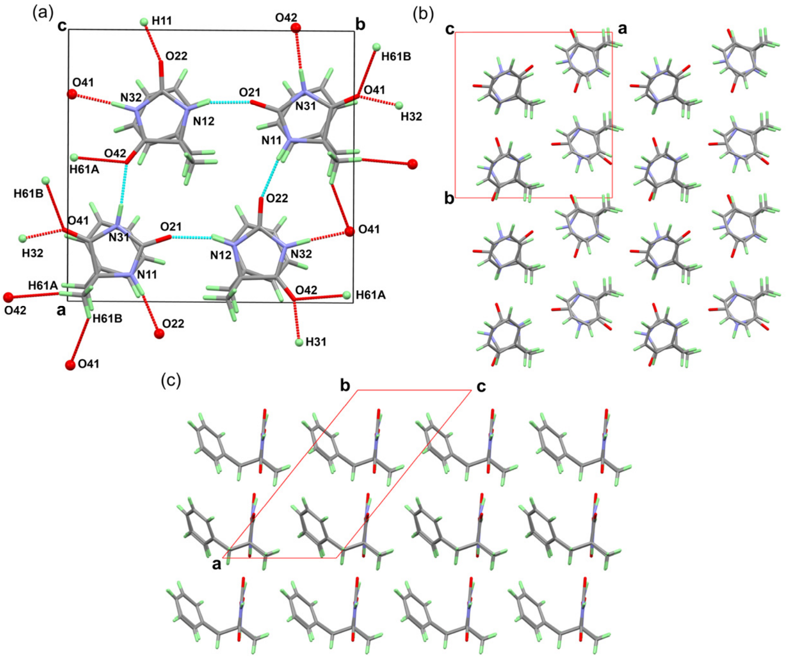

Figure 2. Visualization of the intermolecular hydrogen bonding interactions stabilizing the crystal structure of X—(**a**) and three-dimensional packing of the molecules of X with views perpendicular to *c*-axis (**b**) and *b*-axis (**c**) showing the pseudo layering. Hydrogen atoms are given in light green for clarity.

Table 1. Hydrogen-bond geometry.

D—H···*A*	*D*—H, Å	H···*A*, Å	*D*···*A*, Å	*D*—H···*A*, °
N32—H32···O41 $^{\text{ii}}$	1.02 (3)	1.81 (3)	2.831 (3)	176 (3)
N31—H31···O42 $^{\text{iii}}$	0.91 (4)	1.88 (4)	2.781 (5)	173 (3)
N12—H12···O21	0.91 (4)	1.92 (5)	2.789 (4)	159 (4)
N11—H11···O22 $^{\text{iv}}$	0.92 (5)	1.93 (5)	2.835 (5)	166 (4)
C61—H61*A*···O42 $^{\text{i}}$	0.96 (4)	2.53 (5)	3.409 (5)	153 (3)
C61—H61*B*···O41 $^{\text{iv}}$	0.96 (4)	2.67 (5)	3.444 (5)	137 (2)

Symmetry codes: (i) x, 1 + y, +z; (ii) +x, −1 + y, +z; (iii) −1/2 + x, 1 − y, −1/2 + z; (iv) 1/2 + x, 1 − y, 1/2 + z.

To study the molecular structure, we used the DFT methodology in the gas phase. The computational study was conducted at the B3LYP/6-311++G** level of the theory [33,34], implementing the Gaussian03 suite of programs [35]. DFT methods, and in particular the B3LYP functional in combination with extended basis sets, have proven reliable for structure prediction and frequency calculations of large numbers of species, including molecules, anions, radicals, ions, and complexes [36–39]. The optimized structure is shown in Figure 3.

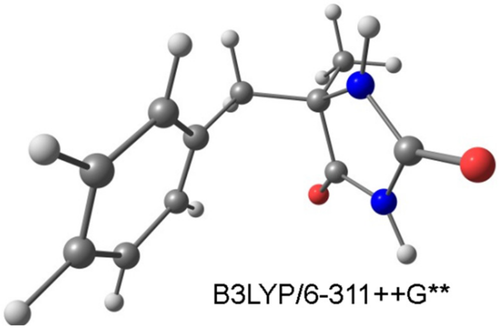

Figure 3. Optimized structure of the compound.

Table 2 presents select experimental and theoretical geometric parameters of the compound.

Table 2. Selected geometric parameters.

Parameters	Exp.	Theor.
	Bond lengths (Å)	
C_{22}-O_{22}	1.21	1.21
C_{22}-N_{12}	1.35	1.37
C_{42}-O_{42}	1.20	1.21
C_{42}-N_{42}	1.33	1.36
C_{52}-C_{62}	1.51	1.53
C_{52}-C_{72}	1.54	1.55
	Angles (°)	
N_{12}-C_{52}-C_{62}	111.7	111.8
N_{12}-C_{52}-C_{72}	111.4	113.2
N_{32}-C_{42}-C_{52}	107.7	106.4
O_{22}-C_{22}-N_{32}	128.6	128.9
O_{42}-C_{42}-N_{32}	125.7	127.2
	Dihedral angles (°)	
C_{42}-C_{52}-C_{72}-C_{82}	−53.4	58.4
C_{62}-C_{52}-N_{12}-C_{22}	−123.8	−119.3
N_{12}-C_{52}-C_{72}-C_{82}	−56.3	53.9

The optimized structural parameters regarding bond lengths and angles agree reasonably well with those obtained by X-ray diffraction. The distances between the atoms do not differ by more than 0.02 Å. A significant deviation is observed when comparing the theoretical data for dihedral angles in the gas phase with those determined experimentally by X-ray structure analysis.

The reason for the observed deviations from the theoretically predicted dihedral angles (which correspond to an isolated molecule in the gas phase) is the presence of moderately strong intermolecular interactions in the solid state.

3. Materials and Methods

Phenylacetone is a trade product. Melting point was determined on BUCHI 535 (BÜCHI Labortechnik AG, Meierseggstrasse 40, Switzerland) melting point system. The IR spectrum was recorded on Thermo Scientific Nicolet iS10 spectrophotometer (Thermo Fisher Scientific, Waltham, MA 02451, USA) in the range of 4000–400 cm^{-1} as Attenuated Total Reflection Fourier Transform Infrared Spectroscopy (ATR-FTIR). ^{1}H and ^{13}C NMR spectra were registered on Bruker Avance 500 (500 MHz) spectrometer in DMSO-d_6 as a solvent. The mass spectrum of the compound was recorded on LC-MS (Thermo Scientific q Exactive Plus—Dionex 3000RSLC).

3.1. Preparation of 5-Methyl-5-Benzyl Hydantoin (Ours Modification)

Phenylacetone (13.4 g, 0.1 mol) was dissolved in a mixture of 60 mL ethanol and 60 mL water. To the solution, we added 7.4 g (0.15 mol) NaCN and 13.2 g (0.15 mol) $(NH_4)_2CO_3$. The solution was heated at 60 °C and stirred for 24 h. After that, the reaction mixture was acidified in a strong ventilation hood with conc. HCl to pH = 6–6.5 and cooled to room temperature. The resulting crystals were filtered off and re-crystallized from 50% ethanol and dried. Yield of recrystallized product was 14.24 g (69.3%). M.p. 228–229 °C [18] M.p. 227–228 °C. IR: 3109; 1748; 1732; 1628; 1575; 1533. ^{1}H NMR (500 MHz, DMSO-d_6): 10.36 (s, 1H, NH-3); 7.98 (s, 1H, NH-1); 7.34 (d, 2H, J = 7 Hz, H-ortho); 6.91 (t, 2H, J = 7 Hz, H-metha); 6.81 (t, 1H, J = 7 Hz, H-para); 3.16, 2.94 (AB quartet, 2H, J = 15.5 Hz, CH_2); 1.32 (s, 3H, CH_3). ^{13}C NMR (125 MHz, DMSO-d_6): 178.0 (C-4); 156.6 (C-2); 137.1 (C_{ar}-CH_2); 127.8, 127.0, 125.7 (C-arom.); 63.3 (C-5); 37.5 (CH_2); 24.1 (CH_3). Mass spectrum: $M + H^+$ = 205.09675 (Figure S3).

3.2. Single-Crystal X-Ray Diffraction Analysis

Colorless block-shaped crystals of 5-Methyl-5-benzyl hydantoin were obtained with slow evaporation from 50% ethanol. A suitable single crystal ($0.35 \times 0.25 \times 0.15$ mm^3) was selected and mounted on a nylon loop using an oil-based cryoprotectant. Diffraction data were collected at 290 K on a SupernovaDual diffractometer equipped with an Atlas CCD detector and micro-focus Mo$K\alpha$ X-ray source (λ = 0.71073). Data were processed with CrysalisPro software ver. 1.171.36.32 [40]. Data were corrected for absorption effects using multi-scan method. The structure was solved with direct methods (ShelxS ver. 2019 [41]) and refined with the full-matrix least-squares method on F^2 (ShelxL 2019/1 [42]) utilizing Olex2 ver. 1.5 graphical user interface [43]. All carbon, nitrogen, and oxygen atoms were located from electron density maps and were refined anisotropically. Hydrogen atoms attached to carbon atoms were placed on calculated positions and refined using the riding model: Ueq = 1.2 for C-$H_{aromatic}$ = 0.93 Å and C-$H_{methylenic}$ = 0.97 Å and Ueq = 1.5 for C-H_{methyl} = 0.96 Å. Nitrogen-bonded hydrogen atoms were placed from electron density maps and refined isotropically. Molecules present in the asymmetric unit (ASU) were visualized using ORTEP-3 ver. 2020.1 software [27]. Illustrations concerning the hydrogen bonding interactions and three-dimensional arrangement of the molecules in the crystal structure were made using CCDC Mercury ver. 4.0 [44]. Data collection and refinement parameters are given in Table S1. Values for bond lengths, bond angles, and torsion angles are given in Tables S2–S4. Complete crystallographic data for the reported structure were deposited in the CIF format with the Cambridge Crystallographic Data Centre as ref. code 2408740. These data can be obtained free of charge via www.ccdc.cam.ac.uk/structures (accessed on 9 December 2024).

4. Conclusions

A different synthetic route was used to synthesize 5-methyl-5-benzyl hydantoin to improve the reaction time, purity, and practical yield compared to the Herbst method. The compound was characterized spectroscopically by IR, ^{1}H, ^{13}C NMR, and mass spectra. The crystal structure of the compound was determined by X-ray diffraction analysis. DFT methodology in the gas phase was used to investigate the molecular structure of the compound. A good agreement has been found between calculated and experimental structural parameters.

Supplementary Materials: Figure S1: Experimental IR spectrum of the compound; Figure S2: ^{1}H NMR spectrum; Figure S3: ^{13}C NMR spectrum of the compound; Figure S4: Mass spectrum of the compound; Table S1: Crystal data and structure refinement for the compound; Table S2: Bond lengths; Table S3: Bond angles; Table S4: Torsion angles; Table S5: Data of ^{1}H and ^{13}C NMR spectra of the compound.

Author Contributions: Conceptualization, R.B. and A.B.; methodology, R.B. and A.B.; software, B.S. and E.C.; formal analysis, E.C., R.B. and B.S.; investigation, E.C., R.B. and B.S.; writing—original draft preparation, R.B. and E.C.; writing—review and editing, E.C. and A.B.; visualization, E.C. and R.R.; supervision, A.B. All authors have read and agreed to the published version of the manuscript.

Funding: This research received no external funding.

Data Availability Statement: Data are contained within the article and Supplementary Materials.

Conflicts of Interest: The authors declare no conflicts of interest.

References

1. Meusel, M.; Gütschow, M. Recent developments in hydantoin chemistry. A Review. *Org. Prep. Proced. Int.* **2004**, *36*, 391–443. [CrossRef]
2. Konnert, L.; Lamaty, F.; Martinez, J.; Colacino, E. Recent advances in the synthesis of hydantoins: The state of the art of a valuable scaffold. *Chem. Rev.* **2017**, *117*, 13757–13809. [CrossRef] [PubMed]
3. Wadghane, S.; Bhor, R.; Shinde, G.; Kolhe, M.; Pooja, R. A review on the some biological activities of the hydantoin derivatives. *J. Drug Deliv. Ther.* **2023**, *13*, 171–178. [CrossRef]
4. Abida, A.M.; Asif, M. Study of some hyndantion derivatives as anticonvulsant agents. *Prog. Chem. Biochem. Res.* **2020**, *3*, 93–104. [CrossRef]
5. Kochetkov, K.A.; Gorunova, O.N.; Bystrova, N. Biologically oriented hybrids of indole and hydantoin derivatives. *Molecules* **2023**, *28*, 602. [CrossRef]
6. Hassanin, M.A.; Mustafa, M.; Hassan, H.A.; Beshr, E.A.M.; Elshennawy, A.T.M.; Aly, O.M. Hydantoin derivatives: A review on their anticancer activities. *Octahedron Drug Res.* **2024**, *4*, 61–74. [CrossRef]
7. Cho, S.H.; Kim, S.H.; Shin, D. Recent applications of hydantoin and thiohydantoin in medicinal chemistry. *Eur. J. Med. Chem.* **2019**, *164*, 517–545. [CrossRef]
8. Kumar, S.A.; Bhaskar, B.L. Spectroscopic and computational approach for the structure—Property relationship of hydantoin drug impurity: 1-methyl-5, 5-diphenylimidazolidine-2,4-dione. *IOP Conf. Ser. Mater. Sci. Eng.* **2019**, *577*, 012180. [CrossRef]
9. Zhu, Q.F.; Pan, Y.H.; Xu, Z.X.; Li, R.M.; Qiu, G.G.; Xu, W.J.; Ke, X.B.; Wu, L.M.; Hu, X.M. Synthesis and potential anticonvulsant activity of new N-3-substituted 5,5-cyclopropanespirohydantoins. *Eur. J. Med. Chem.* **2009**, *44*, 296–302. [CrossRef]
10. Byrtus, H.; Obniska, J.; Czopek, A.; Kaminski, K. Synthesis and anticonvulsant activity of new N-Mannich bases derived from 5-cyclopropyl-5-phenylhydantoins. *Arch. Pharm.* **2011**, *344*, 231–241. [CrossRef]

11. Sondhi, S.M.; Singh, J.; Kumar, A.; Jamal, H.; Gupta, P.P. Synthesis of amidine and amide derivatives and their evaluation for anti-inflammatory and analgesic activities. *Eur. J. Med. Chem.* **2009**, *44*, 1010–1015. [CrossRef] [PubMed]
12. Da Silva Guerra, A.S.H.; Do Nascimento Malta, D.J.; Morais Laranjeira, L.P.; Souza Maia, M.B.; Colaço, N.C.; de Lima, M.D.C.A.; Galdino, S.L.; Da Rocha Pitta, I.; Gonçalves-Silva, T. Anti-inflammatory and antinociceptive activities of indoleeimidazolidine derivatives. *Int. Immunopharm.* **2011**, *11*, 1816–1822. [CrossRef] [PubMed]
13. Stilz, H.U.; Guba, W.; Jablonka, B.; Just, M.; Klingler, O.; Konig, W.; Wehner, V.; Zoller, G. Discovery of an orally active non-peptide fibrinogen receptor antagonist based on the hydantoin scaffold. *J. Med. Chem.* **2001**, *44*, 1158–1176. [CrossRef] [PubMed]
14. Jung, M.E.; Ouk, S.; Yoo, D.; Sawyers, C.L.; Chen, C.; Tran, C.; Wongvipat, J. Structure-activity relationship for thiohydantoin androgen receptor antagonists for castration-resistant prostate cancer (CRPC). *J. Med. Chem.* **2010**, *53*, 2779–2796. [CrossRef]
15. Malancona, S.; Altamura, S.; Filocamo, G.; Kinzel, O.; Hernando, J.I.M.; Rowley, M.; Scarpelli, R.; Steinkühler, C.; Jones, P. Identification of MK-5710 ((8aS)-8-a-methyl-1,3-dioxo-2-[(1S,2R)-2-phenylcyclopropyl]-N-(1-phenyl-1H-pyrazol-5-yl)hexahydroimidazo [1,5-a]pyrazine-7(1H)-carboxamide), a potent smoothened antagonist for use in Hedgehog pathway dependent malignancies, Part 1. *Bioorg. Med. Chem. Lett.* **2011**, *21*, 4422–4428. [CrossRef]
16. Kim, D.; Wang, L.; Caldwell, C.G.; Chen, P.; Finke, P.E.; Oates, B.; MacCoss, M.; Mills, S.G.; Malkowitz, L.; Gould, S.L.; et al. Design, synthesis, and SAR of heterocycle-containing antagonists of the human CCR5 receptor for the treatment of HIV-1 infection. *Bioorg. Med. Chem. Lett.* **2001**, *11*, 3103–3106. [CrossRef]
17. Romine, J.L.; St. Laurent, D.R.; Leet, J.E.; Martin, S.W.; Serrano-Wu, M.H.; Yang, F.K.; Gao, M.; O'Boyle, D.R.; Lemm, J.A.; Sun, J.H.; et al. Inhibitors of HCV NS5A: From iminothiazolidinones to symmetrical stilbenes. *ACS Med. Chem. Lett.* **2011**, *2*, 224–229. [CrossRef]
18. Trišović, N.; Timić, T.; Divljaković, J.; Rogan, J.; Poleti, D.; Savić, M.M.; Ušćumlić, G. Synthesis, structural and biological characterization of 5-phenylhydantoin derivatives as potential anticonvulsant agents. *Monatsh. für Chem.* **2012**, *143*, 1451–1457. [CrossRef]
19. Hashmi, I.A.; Aslam, A.; Ali, S.K.; Ahmed, V.-U.; Ali, F.I. Synthesis of hydantoins, thiohydantoins, and glycocyamidines under solvent-free conditions. *Synth. Commun.* **2010**, *40*, 2869–2874. [CrossRef]
20. Bucherer, H.T.; Fischbeck, H.T. Hexahydrodiphenylamine and its derivatives. *J. Prakt. Chem.* **1934**, *140*, 69–89.
21. Bergs, Hydantoinderivate. *Ger. Pat.* 566094 **1929**. *Chem. Abstr.* **1933**, *27*, 1001.
22. Bucherer, H.T.; Steiner, W.J. Über die reaktionen der α–oxy und α–aminonitrilen. Synthese von hydantoinen. *Prakt. Chem.* **1934**, *140*, 291.
23. Bucherer, H.T. Über die bildung substituiereter hydantoine aus aldehyden und ketonen. *Prakt. Chem.* **1934**, *141*, 5. [CrossRef]
24. Urech, F. Ueber lacturaminsäure und lactylharnstoff. *Liebigs Ann.* **1873**, *165*, 99–103. (In German) [CrossRef]
25. Herbst, R.; Johnson, T. Researches on hydantoins. L.[1] The synthesis of hydantoins possessing the properties of hypnotics. *J. Amer. Chem. Soc.* **1932**, *54*, 2463. [CrossRef]
26. Cherneva, E.; Buyukliev, R.; Burdjiev, N.; Michailova, R.; Bakalova, A. Pd(II) and Pd(IV) complexes with new hydantoin based ligand. Synthesis, characterization, computational and pharmacological studies. *Bulg. Chem. Commun.* **2018**, *50*, 237–242.
27. Farrugia, L.J. Wingx and Ortep for Windows: An Update. *J. Appl. Crystallogr.* **2012**, *45*, 849–854. [CrossRef]
28. Chattopadhyay, B.; Mukherjee, A.K.; Narendra, N.; Hemantha, H.P.; Sureshbabu, V.; Helliwell, M.; Mukherjee, M. Supramolecular architectures in 5,5′-substituted hydantoins: Crystal structures and hirshfeld surface analyses. *Cryst. Growth Des.* **2010**, *10*, 4476–4484. [CrossRef]
29. Lazić, A.; Radovanović, L.; Rogan, J.; Valentić, N.; Janjić, G.; Đorđević, I.; Trišović, N. Exploring the supramolecular profile of 5-phenylhydantoins. *Cryst. Eng. Comm.* **2023**, *25*, 3637–3654. [CrossRef]
30. Giunchi, A.; Rivalta, A.; Bedoya-Martínez, N.; Schrode, B.; Braun, D.; Werzer, O.; Venuti, E.; Della Valle, R.G. Surface induced phenytoin polymorph. 1. Full structure solution by combining grazing incidence X-ray diffraction and crystal structure prediction. *Cryst. Growth Des.* **2019**, *19*, 6067–6073. [CrossRef]
31. Brown, I.D. On the geometry of O–H··· O hydrogen bonds. *Acta Crystallogr. Sect. A Found. Crystallogr.* **1976**, *32*, 24–31. [CrossRef]
32. Taylor, R.; Kennard, O.; Versichel, W. Geometry of the nitrogen-hydrogen...oxygen-carbon (NH...O:C) hydrogen bond. 2. Three-center (bifurcated) and four-center (trifurcated) bonds. *J. Am. Chem. Soc.* **1984**, *106*, 244–248. [CrossRef]
33. Stephens, P.J.; Devlin, F.J.; Chabalowski, C.F.; Frisch, M.J. Ab Initio calculation of vibrational absorption and circular dichroism spectra using Density Functional Force Fields. *J. Phys. Chem.* **1994**, *98*, 11623–11627. [CrossRef]
34. Lee, C.; Yang, W.; Paar, R.G. Development of the Colle-Salvetti correlation-energy formula into a functional of the electron density. *Phys. Rev. B* **1988**, *37*, 785–789. [CrossRef] [PubMed]
35. Frisch, M.J.; Trucks, G.W.; Schlegel, H.B.; Scuseria, G.E.; Robb, M.A.; Cheeseman, J.R.; Montgomery, J.A.; Vreven, T.; Kudin, K.N.; Burant, J.C.; et al. *Gaussian 03, Revision C.02*; Gaussian Inc.: Wallingford, CT, USA, 2004.
36. Daskalova, L.I.; Velcheva, E.A.; Binev, I.G. Changes in the IR spectra and structures of pyridine-3-carboxamides-d_0 and -d_2 caused by their conversion into azanions-d_0 and -d_1: Experimental and computational studies. *J. Mol. Struct.* **2007**, *826*, 198–204. [CrossRef]

37. Yancheva, D.; Stoyanov, S.; Anichina, K.; Nikolova, S.; Velcheva, E.; Stamboliyska, B. Combined infrared spectroscopic and computational study on simpler capsaicin derivatives and their anion intermediates in the scavenging of free radicals. *Chem. Phys.* **2020**, *535*, 110763. [CrossRef]
38. Tachikawa, H.A.; Kawabata, H. Structures and electronic states of permethyloligosilane radical ions with all-trans form $Sin(CH_3)_{2n+2(\pm)}$ (n = 2–6): A Density Functional Theory study. *J. Chem. Theory Comp.* **2007**, *3*, 184–193. [CrossRef]
39. Stoyanov, S.; Yancheva, D.; Stamboliyska, B. DFT study on IR spectral and structural changes caused by the conversion of substituted benzophenones into ketyl radicals. *Comput. Theor. Chem.* **2014**, *1046*, 57–63. [CrossRef]
40. Sheldrick, G.M. Crystal Structure Refinement with Shelxl. *Acta Crystallogr. Sect. C* **2015**, *71*, 3–8. [CrossRef]
41. Rigaku, O. *Crysalis PRO*; Rigaku Oxford Diffraction: Yarnton, UK, 2015.
42. Sheldrick, G.M. A short history of shelx. *Acta Crystallogr. Sect. A Found. Crystallogr.* **2008**, *64*, 112–122.
43. Dolomanov, O.V.; Bourhis, L.J.; Gildea, R.J.; Howard, J.A.K.; Puschmann, H. Olex2: A Complete structure solution, refinement and analysis program. *J. Appl. Crystallogr.* **2009**, *42*, 339–341. [CrossRef]
44. Macrae, C.F.; Sovago, I.; Cottrell, S.J.; Galek, P.T.A.; McCabe, P.; Pidcock, E.; Platings, M.; Shields, G.P.; Stevens, J.S.; Towler, M. Mercury 4.0: From visualization to analysis, design and prediction. *J. Appl. Crystallogr.* **2020**, *53*, 226–235. [CrossRef] [PubMed]